

# Signalling pathways involved in ribonuclease-7 expression

Imran Mohammed · Aaron Yeung ·  
Asiya Abedin · Andrew Hopkinson ·  
Harminder S. Dua

Received: 10 November 2009 / Revised: 22 September 2010 / Accepted: 27 September 2010 / Published online: 22 October 2010  
© Springer Basel AG 2010

**Abstract** Antimicrobial peptides are host defence molecules that play a potential role in preventing infection at the epithelial surfaces. Ribonuclease (RNase)-7 has been shown to possess a broad spectrum of microbicidal activity against various pathogens. Here, we demonstrate that RNase-7 protein is localised to the superficial layers of ocular surface cells and increased in response to interleukin (IL)-1 $\beta$ , suggesting an active role during inflammation related to ocular surface infection. Signal transduction pathways involved in RNase-7 expression are unknown. Involvement of transforming growth factor  $\beta$ -activated kinase-1 (TAK-1) activated nuclear factor kappa B (NF- $\kappa$ B) and mitogen-activated protein kinase (MAPK) pathway molecules [c-Jun N-terminal kinase (JNK), extracellular signal-regulated kinase (ERK) and p38] were studied because of their importance in infection and inflammation. Blocking the MAPKs resulted in inhibition of RNase-7 expression in response to IL-1 $\beta$ . However, RNase-7 induction by IL-1 $\beta$  was not affected by inhibiting the NF- $\kappa$ B signalling pathway. In conclusion, our results

indicate that RNase-7 expression is specifically mediated via MAPKs but not NF- $\kappa$ B signalling pathways.

**Keywords** Ribonuclease-7 (RNase-7) ·  
TGF $\beta$ -activated kinase-1 (TAK-1) ·  
Nuclear factor  $\kappa$ B (NF- $\kappa$ B) · Interleukin-1 $\beta$  (IL-1 $\beta$ ) ·  
Mitogen-activated protein kinases (MAPKs)

## Abbreviations

RNase-7	Ribonuclease-7
HBD-2	Human beta defensin-2
OS	Ocular surface
NAI	NF- $\kappa$ B activation inhibitor
SC-514	a IKK-2 inhibitor
hCEC	Human corneal epithelial cell line
TAK-1	TGF $\beta$ -activated kinase-1
NF- $\kappa$ B	Nuclear factor $\kappa$ B
IL	Interleukin
TNF	Tumour necrosis factor
ERK	Extracellular signal-regulated kinases
JNK	c-Jun N-terminal kinases
MAPKs	Mitogen-activated protein kinases
ATF2	Activating transcription factor 2

**Electronic supplementary material** The online version of this article (doi:10.1007/s00018-010-0540-2) contains supplementary material, which is available to authorized users.

I. Mohammed · A. Yeung · A. Abedin · A. Hopkinson ·  
H. S. Dua

Larry A Donoso Laboratory for Eye Research,  
Division of Ophthalmology and Visual Sciences,  
University Hospital, Nottingham NG7 2UH, UK

H. S. Dua (✉)  
Division of Ophthalmology and Visual Sciences,  
Eye and ENT Building, Queens Medical Centre Campus,  
Derby Road, Nottingham NG7 2UH, UK  
e-mail: Harminder.Dua@nottingham.ac.uk

## Introduction

The ocular surface (OS) is an integral part of the mucosal immune system and like other mucosal surfaces has evolved several defence mechanisms to counter microbial infection. In particular, cytokines, chemokines and antimicrobial peptides (AMPs) play a seminal protective role at the OS epithelium [1, 2]. Different classes of AMPs exist as naturally occurring eukaryotic antibiotic analogues with

broad-spectrum activity against bacteria, fungi, protozoa, mycobacteria and enveloped viruses [3, 4]. Studies of AMPs have recently focused on the ribonuclease A superfamily in the background of its dynamic evolutionary history [5]. Of the members of this superfamily, RNase-7 was demonstrated to possess a broad spectrum of activity at low micro-molar concentrations against pathogenic bacteria including vancomycin-resistant *Enterococcus faecium* [6–8]. In response to heat-killed bacteria, UV radiation and proinflammatory cytokines, increased RNase-7 mRNA expression was exhibited in primary keratinocytes [6, 9]. In addition RNase-7 mRNA levels were also shown to be increased in skin biopsies of psoriasis and atopic dermatitis [10]. Reithmayer and co-workers [11] have shown that the immunoreactivity of RNase-7 in fresh and organ-cultured normal human scalp skin increases when treated with lipopolysaccharide (LPS) and flagellin. However, RNase-7 expression at the OS epithelium has not been previously reported. Here, we demonstrated the expression of RNase-7 in cells obtained from the cornea and conjunctiva of the human eye and further report, for the first time, on signalling pathways involved in such expression using an SV (Simian virus)-40 transformed human corneal epithelial cell line (hCEC) model. These pathways have not been elucidated for RNase-7 in any tissue thus far. Our discovery of RNase-7 and its signalling pathways expands the current knowledge of AMP defence.

Interleukin-1 $\beta$  plays an essential role in innate immunity by eliciting both cytokines and AMPs. IL-1 $\beta$  binds to the IL-1 receptor (IL-1R) and initiates the activation of a key signalling protein, transforming growth factor  $\beta$ -activated kinase-1 (TAK-1). Subsequently, TAK-1 leads to activation of transcription factors such as nuclear factor kappa-B (NF- $\kappa$ B) and activator protein-1 (AP-1). Eventually, these transcription factors initiate the expression of genes involved in the host immune response [12–15]. By blocking the various signalling pathways with selective inhibitory peptides and small-interfering RNA (siRNA), we have demonstrated the direct involvement of TAK-1-mediated MAPK pathways, but not NF- $\kappa$ B, in upregulation of RNase-7 expression by IL-1 $\beta$ .

## Materials and methods

### Reagents and antibodies

Recombinant human IL-1 $\beta$ , NF- $\kappa$ B inhibitors, SC-514 and NAI (NF- $\kappa$ B activation inhibitor) and MAPK inhibitors, SB203580, PD98059 and SP600125 were purchased from Calbiochem. Polyclonal rabbit anti-human RNase-7 was purchased from Atlas Antibodies. Monoclonal rabbit anti-human antibodies against TAK-1, p38, JNK, ERK,

NF- $\kappa$ B/p65, I $\kappa$ B- $\alpha$ , c-Jun and ATF2 were obtained from Cell Signalling Technologies. The polyclonal rabbit anti-human  $\beta$ -actin antibody (Ab) was purchased from Serotec.

### SV40-transformed human corneal epithelial cell lines (hCECs)

Cells were maintained in Epilife medium (Cascade Biologics) supplemented with human keratinocyte growth supplement (HKGS) and gentamicin/amphotericin B solution (Cascade Biologics). Cells ( $1 \times 10^5$  cells/well) were cultured in six-well plates and incubated in humidified conditions (5% CO<sub>2</sub>) at 37°C until optimum growth was achieved. Before treatment cells were starved overnight in HKGS free media.

### Extraction of whole cell, cytoplasmic and nuclear proteins

Human corneal epithelial cell lines were grown to confluence and treated with inhibitors at different doses prior to treatment with IL-1 $\beta$ . The most suitable time point and concentration not harmful to the cells were deduced. Whole cell lysates were extracted using mixture of 1 $\times$  NuPAGE LDS sample buffer (Invitrogen) and 0.5 M dithiothreitol (DTT; Sigma). The protein content of the lysates was determined using a 2D Quant kit (Amersham Biosciences) with bovine-serum albumin as a standard. The nuclear and cytoplasmic proteins were extracted according to the manufacturer's instructions using the Nuclear/Cytosol Fractionation kit (Bio Vision). The protein extracts were then quantified and stored at  $-80^\circ\text{C}$  until analysed.

### Western blot protocol

Western blot (WB) was carried out according to the established technique. The protein lysates were resolved on NuPAGE 12% Bis-Tris gel (Invitrogen) and were transferred onto polyvinylidene difluoride (PVDF) membranes (Millipore). The membranes were blocked for 1 h at room temperature using Tris-buffered saline, pH 8.0 (Sigma), 0.05% v/v Tween 20 (Promega) and 5% w/v non-fat dried milk powder followed by incubation with the primary monoclonal Ab overnight at 4°C to detect total or phosphorylated proteins. The blots were then incubated with alkaline phosphatase-conjugated secondary Ab to detect the primary Ab and then developed with premixed alkaline phosphatase chromogen kit (BCIP/NBT; Sigma).

### Isolation of total RNA and cDNA synthesis

Total RNA was extracted from cell-culture samples using the RNeasy Mini kit (Qiagen) according to the

manufacturer's instructions. Then 1 µg of RNA from cultured cells was reverse transcribed into cDNA using the Quantitect Reverse Transcription Kit (Qiagen).

#### Quantitative real-time PCR (qPCR)

Quantitative real-time PCR analysis was performed to measure the relative abundance of RNase-7 mRNA. Custom-made Taqman assays (Applied Biosystems) were used as indicated in Online Resource 6. qPCR reactions were run on eight-strip optical tubes (Stratagene) in the Mx3005p real-time PCR system (Stratagene). The data obtained from the machine were further analysed to calculate the relative quantity of mRNA.

#### RNAi silencing

Cells ( $8 \times 10^4$ ) were seeded onto 12-well plates and grown overnight. In brief, 1 µM of gene-specific siRNA (Table SI-1) or 10 µM of negative control siRNA and 2 µl of *INTERFERin* transfection reagent (Polyplus) were premixed in 200 µl Opti-MEM-1 (Invitrogen) by gentle vortexing and then incubated for 10 min at room temperature. During complex formation, growth medium was removed from the cells and replaced by 800 µl of Opti-MEM-1 per well; then the premix complex was overlaid drop-wise with gentle rocking. The final siRNA concentration was 1 nM for gene-specific siRNA or 10 nM for negative control siRNA in 1 ml of Opti-MEM-1. The plates were incubated for 24 h in humidified conditions. siRNAs used in this study are detailed in Online Resource 7.

#### RNAi Knockdown efficiency

Following hCEC ( $4 \times 10^4$ ; 24-well plate) treatment with various concentrations of gene-specific Silencer select siRNA (Online Resource 6) or 10 µM of negative control siRNA in the presence of 1 µl of *INTERFERin* transfection reagent, total RNA extraction and reverse transcription were performed. Quantitative PCR analysis was carried out on the Mx3005p (Stratagene) and using gene-specific Taqman assays against indicated target molecules (Online Resource 7). Data were normalised with the level of 18 s rRNA expression in each sample. Knockdown efficiency was measured using qPCR (Online Resource 2).

#### Negative control siRNA transfection efficiency

To evaluate the transfection efficiency of siRNA into hCECs, we used FAM-labelled Negative Control siRNA (Ambion). Cells ( $2 \times 10^4$ ) seeded onto four-well chamber slide (Lab-tek) overnight before treatment with fluorescently

labeled siRNA for 24 h in the presence of *INTERFERin*<sup>TM</sup> transfection reagent (Polyplus). This was followed by fixing with 4% paraformaldehyde and then permeabilisation with 0.5% Triton-X. The counterstaining was performed with 4',6-diamidino-2-phenylindole (DAPI), and cells were examined using a Nikon Alphaphot-2 fluorescent microscope (Nikon). Transfection efficiency was measured using the IF technique (Online Resource 3).

#### Immunofluorescence staining

Immunostaining was performed for detection of RNase-7 protein at the ocular surface and in cultured corneal epithelium using established techniques. Briefly, the ocular tissue was collected from the human cadaver eyes after obtaining local ethics committee approval and prior consent from the donors' relatives, via the UK eye banking system. The cadaver ocular tissue was processed within 48 h of death under aseptic conditions. A 15-mm trephine was used to dissect the corneoscleral button maintaining a 3-mm frill of conjunctiva around the limbus. The button was divided into eight segments and then snap frozen with OCT (optimum cutting temperature) compound (Tissue Tek). The ocular tissue (7-µm-thick sections) was fixed in acetone. Alternatively, cells ( $2 \times 10^4$ ) seeded onto four-chamber slides (Lab-Tek) were fixed with 4% paraformaldehyde and then permeabilised with 0.5% Triton-X. Samples were then blocked with normal goat serum (1:10) for 30 min followed by incubation with primary Ab against RNase-7 (dilution, 1:100; rabbit; Atlas Antibodies) overnight at 4°C. Samples were washed and incubated with secondary Ab Alexa Fluor 555 (anti-rabbit; Invitrogen) for 1 h. The counterstaining was performed with 4', 6-diamidino-2-phenylindole (DAPI) and examination performed using a Nikon Alphaphot-2 fluorescent microscope (Nikon). Refer to the Electronic Supplemental Material (ESM), Online Resource 3, for staining of positive control human tonsil tissue and negative control siRNA-treated hCECs.

#### Measurement of cytokine production

Cells were treated with different concentrations of inhibitors prior to stimulation with IL-1β. The culture supernatants were collected, and the concentration of key cytokines in a single analyte was measured using a Becton-Dickinson (BD) Cytometric Bead Array kit (BD Biosciences) according to the manufacturer's instructions. Briefly, the standard curves were generated from the serially diluted standards provided in the kit. The test samples were prepared by mixing 50 µl each of capture beads mix (PE-conjugated anti-human), test analyte and PE detection reagent and then incubated for 3 h at RT.

Following incubation, the samples were washed, pelleted and then reconstituted in 300  $\mu$ l of wash buffer before analysis on the BD-LSR II flow cytometer system (BD Biosciences).

### Statistical analysis

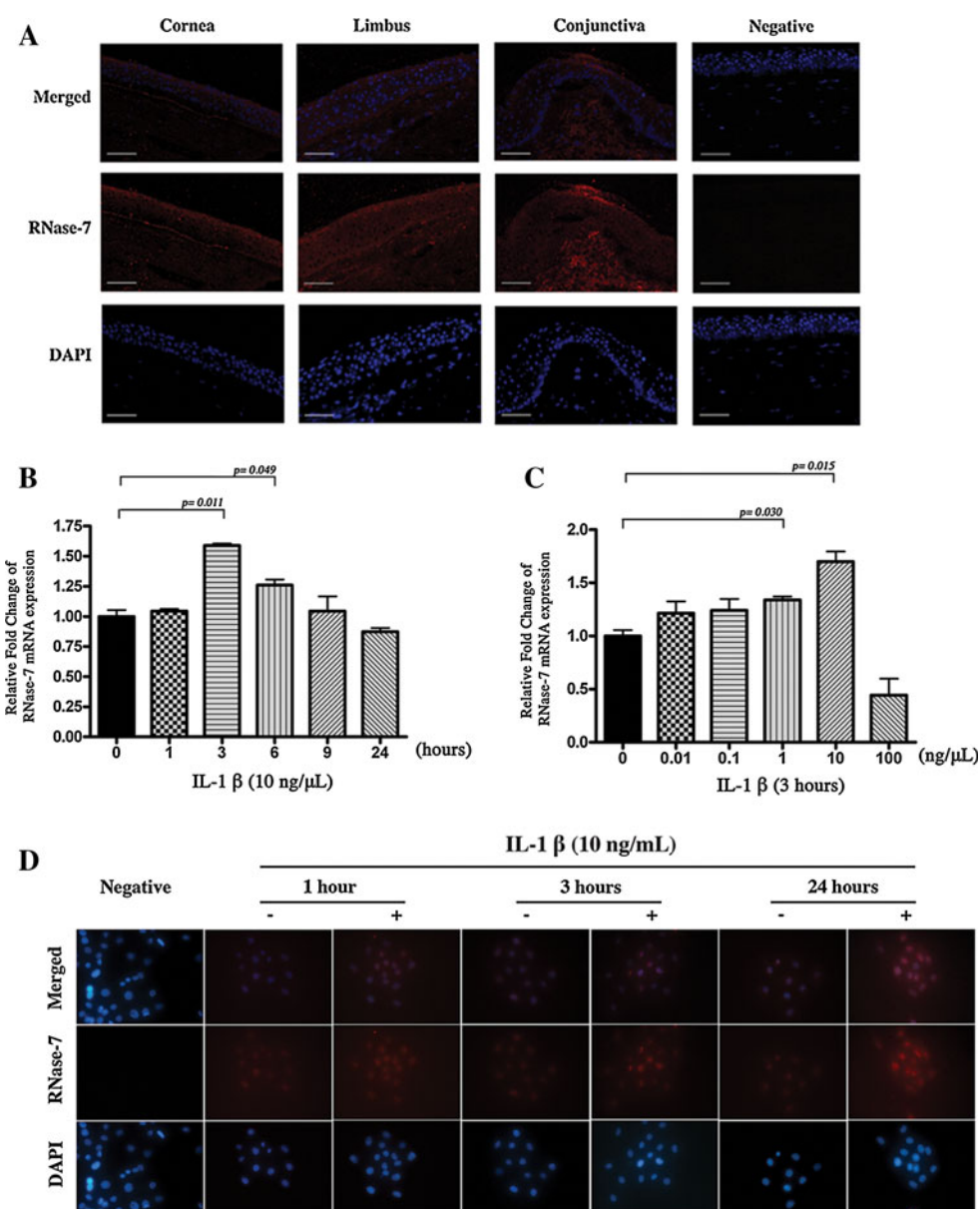
The qPCR data were statistically analysed using SPSS 16.0v software (IBM). The statistical significance was set at  $p \leq 0.05$ . Student's *t*-test was used for statistical analysis of IL-1 $\beta$ -induced RNase-7 expression in hCEC before or after treatment with various inhibitors or gene-specific siRNAs.

## Results

### RNase-7 expression in human OS epithelial cells

To examine the localisation of RNase-7 at the OS, we performed immunofluorescence analysis of intact cornea, limbus and conjunctival tissue. Constitutive expression of RNase-7 was demonstrated in all regions of the OS epithelium (Fig. 1a). The superficial layers of the corneal epithelium and all the layers of the limbus showed high expression of RNase-7 protein. Intriguingly, the conjunctiva demonstrated variable expression of RNase-7, being concentrated in some areas and absent in others. Human

**Fig. 1** In-vitro expression of RNase-7 in human ocular surface. **a** Localisation of RNase-7 protein at OS. The upper panel displays merged images of both RNase-7 (red) and nuclei (DAPI blue) staining. Negative control staining showed no immunoreactive staining. Scale bar: 100  $\mu$ M. **b–d** Effect of IL-1 $\beta$  on RNase-7 expression. **b** Cells were incubated with IL-1 $\beta$  for indicated time points, and qPCR analysis was performed. **c** Cells were treated with different concentrations of IL-1 $\beta$  for 3 h. RNase-7 mRNA levels were analysed by qPCR. Data represent means  $\pm$  SEM of triplicate samples repeated three times.  $p < 0.05$ . **d** Cells were incubated for indicated times with (+) or without (–) IL-1 $\beta$  and were then stained for RNase-7. Scale bar: 100  $\mu$ M. All data are representative of three independent experiments



tonsil, which was used as positive control, also demonstrated the presence of RNase-7 protein (see ESM; Online Resource 1).

### IL-1 $\beta$ modulates RNase-7 expression

Pro-inflammatory cytokine-mediated RNase-7 induction has been previously reported in keratinocytes [6]. To determine whether IL-1 $\beta$  has any effect on low basal regulation of RNase-7 mRNA, the hCECs were treated with IL-1 $\beta$  (10 ng/ml) for various durations (1, 3, 6, 9 and 24 h). A modest increase of RNase-7 transcript levels was observed within 1 h with maximum levels detected at 3 h (Fig. 1b). The initial increase was followed by a time-dependent decrease in transcript levels with minimal expression detected at 24 h. We next investigated the effect of different concentrations of IL-1 $\beta$  on RNase-7 mRNA expression. Incubation of hCECs for 3 h with IL-1 $\beta$  (0.01, 0.1, 1, 10 and 100 ng/ml) resulted in a dose-dependent increase in RNase-7 mRNA with a maximum level detected at a concentration of 10 ng/ml of IL-1 $\beta$  (Fig. 1c). This was followed by a rapid decline in RNase-7 mRNA expression at higher concentration (100 ng/ml).

Furthermore, to examine the effect of IL-1 $\beta$  on RNase-7 protein expression, immunostaining was performed. Treatment with IL-1 $\beta$  (10 ng/ml) for different durations showed maximal levels of RNase-7 protein after 24 h (Fig. 1d). These results indicate a rapid response role of RNase-7 as part of the immediate host response to inflammation or infection.

TAK-1 plays a central role in modulation of RNase-7 expression

In response to different stimuli, TAK-1 is involved in the activation of the immune responses. However, there are no reports available on TAK-1 involvement in OS host defence. To investigate the role of TAK-1 in the IL-1 $\beta$  pathway, hCECs were treated with IL-1 $\beta$  (10 ng/ml) for different durations (5, 15, 30, 60 and 120 min). Western blotting was performed using monoclonal antibody (mAb) against both phosphorylated and unphosphorylated forms of TAK-1. As shown in Fig. 2a, increased phosphorylation of TAK-1 was noted at 15 min with less or no phosphorylation detected after 60 min.

To elucidate the role of TAK-1 in activation of both NF- $\kappa$ B and MAPK pathways in response to IL-1 $\beta$ , cells were incubated with pre-optimised TAK-1 siRNA (see ESM; Online Resource 2A; 1 nM) and negative control siRNA (10 nM) for 24 h prior to IL-1 $\beta$  treatment (10 ng/ml; 30 min). As shown in Fig. 2b, silencing of TAK-1 in hCECs resulted in reduced phosphorylation of I $\kappa$ B- $\alpha$ , ERK1/2, JNK and p38 compared to negative control, suggesting a direct role of TAK-1. We next examined the role of TAK-1 in RNase-7 induction. Silencing of TAK-1 (1 nM; 24 h) prior to IL-1 $\beta$  treatment (10 ng/ml; 3 h) significantly reduced the RNase-7 mRNA expression ( $p < 0.001$ ) in hCECs (Fig. 2c). Similarly, as shown in Fig. 2d, RNase-7 protein was also attenuated in TAK-1 siRNA-treated hCECs compared to negative control. These results indicate the central role of TAK-1 in IL-1 $\beta$ -induced RNase-7 expression.

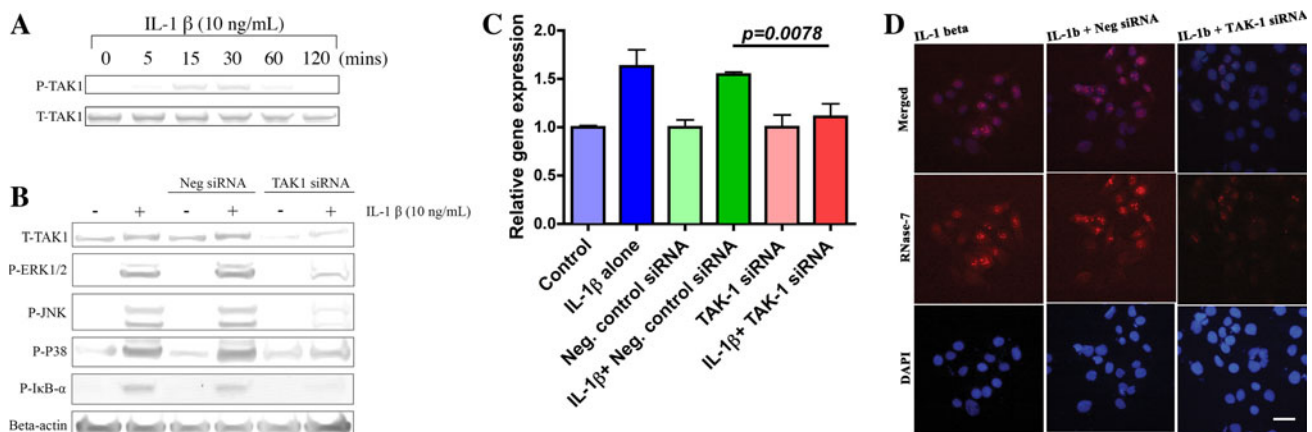


**Fig. 2** Transforming growth factor  $\beta$ -activated kinase-1 plays a central role in modulation of RNase-7 expression. **a** Rapid induction of TAK-1 by IL-1 $\beta$ . Cells treated with IL-1 $\beta$  for indicated time points and then cell lysates were prepared and analysed by WB. **b** TAK-1-dependent regulation of NF- $\kappa$ B and MAPKs in response to IL-1 $\beta$ . Cells transfected without (–) or with (+) TAK-1 siRNA or negative control siRNA were incubated with IL-1 $\beta$  and were then analysed with indicated Abs. **c**, **d** Knockdown of TAK-1 suppresses IL-1 $\beta$  induced RNase-7 expression. **c** Role of IL-1 $\beta$ /TAK-1 axis in RNase-7

mRNA expression. Following transfection without or with indicated siRNA, hCECs were incubated in the presence or absence of IL-1 $\beta$  for 3 h. RNase-7 mRNA was analysed by qPCR and presented as mean value  $\pm$  SEM;  $n = 3$ . The  $p$  value corresponds to the significance relative to the negative control. **d** Reduction in IL-1 $\beta$  induced RNase-7 protein levels in TAK-1 siRNA transfected hCECs. Cells transfected without or with indicated siRNA prior to incubation with IL-1 $\beta$  for 24 h were stained with RNase-7 antibody (red middle panel) and DAPI (blue lower panel). Scale bar 100  $\mu$ M



### RNase-7 expression is independent of NF- $\kappa$ B signalling

Nuclear factor  $\kappa$ B plays an essential role in the expression of numerous genes, in response to IL-1 $\beta$  [12]. To assess the effect of IL-1 $\beta$  on NF- $\kappa$ B activation in hCECs, the degradation of I $\kappa$ B- $\alpha$  and subsequent nuclear translocation of NF- $\kappa$ B were studied. In response to IL-1 $\beta$ , total-I $\kappa$ B- $\alpha$  degradation in cytoplasmic extracts and concurrent NF- $\kappa$ B nuclear translocation became apparent at 5 min and prominent at 15 min (Fig. 3a). Next, we examined the efficacy of two pharmacological inhibitors of NF- $\kappa$ B, NAI (NF- $\kappa$ B activation inhibitor) and SC-514 (IKK-2 inhibitor). Pre-treatment of hCECs with NAI and SC-514 (10  $\mu$ M each; 30 min) prior to IL-1 $\beta$  exposure resulted in reduced phosphorylation of I $\kappa$ B- $\alpha$  in cytoplasm and subsequent attenuation of NF- $\kappa$ B nuclear translocation (Fig. 3b, c), suggesting the involvement of NF- $\kappa$ B in the cellular response to IL-1 $\beta$ .

To elucidate the function of NF- $\kappa$ B in IL-1 $\beta$  induced RNase-7 levels, hCECs were incubated with different

concentrations of NAI (0.1, 1 and 10  $\mu$ M) and SC-514 (1, 10 and 100  $\mu$ M) for 30 min preceding IL-1 $\beta$  treatment (10 ng/ml) for 3 h. Interestingly, inhibition of NF- $\kappa$ B in dose-dependent fashion with NAI and SC-514 showed no effect on RNase-7 mRNA levels in IL-1 $\beta$ -treated hCECs (Fig. 3d). Similarly, as shown in Fig. 3e, blocking of the NF- $\kappa$ B pathway with NAI and SC-514 (10  $\mu$ M; 30 min each) prior to IL-1 $\beta$  treatment (10 ng/ml; 24 h) has demonstrated no effect on RNase-7 protein expression.

To validate our above experiments, we investigated the effect of blocking on known targets of the NF- $\kappa$ B pathway: I $\kappa$ B- $\alpha$  (mRNA), TNF- $\alpha$  (both mRNA and protein), IL-6 (protein) and IL-8 (protein). Inhibition of the NF- $\kappa$ B pathway with NAI and SC-514, respectively, prior to IL-1 $\beta$  treatment has shown both reduction in mRNA expression of I $\kappa$ B- $\alpha$  and TNF- $\alpha$  (see ESM, Online Resource 4) and protein secretion of IL-6, IL-8 and TNF- $\alpha$  (see ESM, Online Resource 5), respectively.

In an inactive form, the hetero- or homo-dimer of NF- $\kappa$ B family subunits (p65/p50 or p50/p50) typically binds to

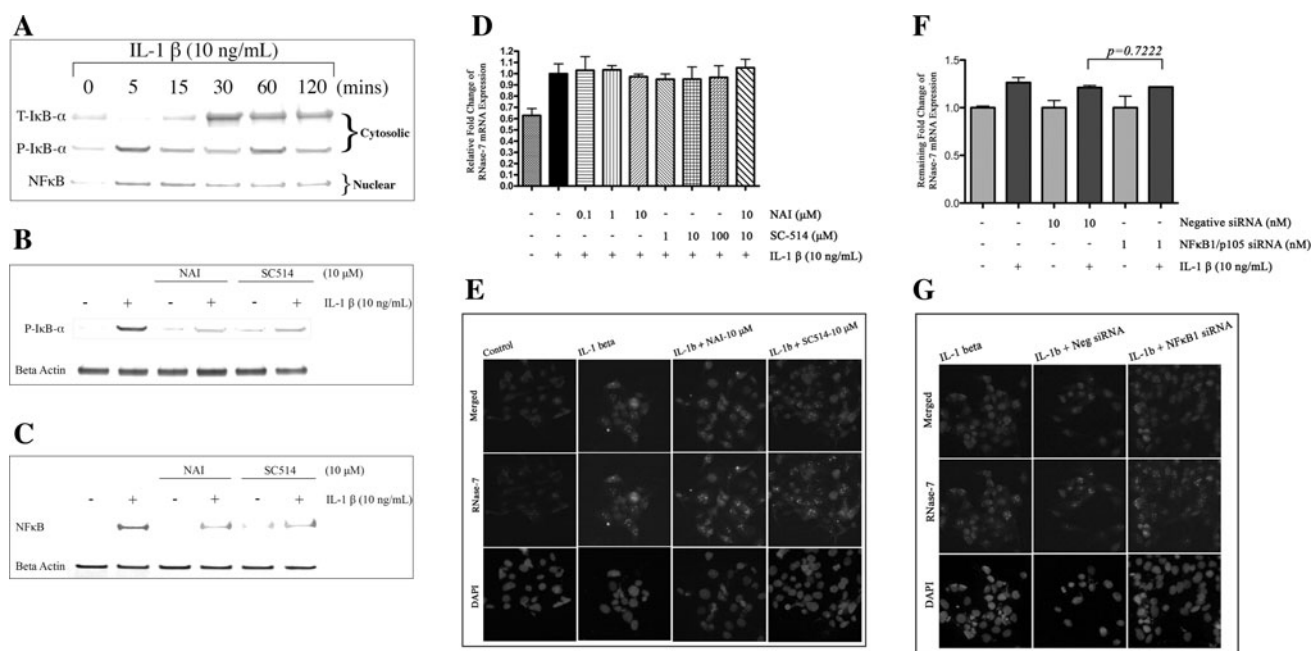


**Fig. 3** RNase-7 expression is independent of NF- $\kappa$ B signalling pathway in hCECs. **a** Activation of NF- $\kappa$ B signalling by IL-1 $\beta$ . Cells were treated with IL-1 $\beta$  for the indicated times. The specified fractions were analysed using WB. **b, c** Suppression of IL-1 $\beta$  activated NF- $\kappa$ B pathway. **b** NAI and SC-514 reduce IL-1 $\beta$ -induced I $\kappa$ B- $\alpha$  phosphorylation. Cytosolic extract was prepared and analysed using WB. **c** Reduced nuclear translocation of NF- $\kappa$ B/p65 in IL-1 $\beta$ -treated hCECs after blocking. Nuclear lysates were prepared as indicated in SI and then analysed using WB. **d, e** Suppression of NF- $\kappa$ B does not effect IL-1 $\beta$  induced RNase-7 expression. **d** NAI and SC-514 do not reduce RNase-7 mRNA expression in IL-1 $\beta$ -treated hCECs. Cells pretreated without or with indicated inhibitors at various concentrations were incubated in the presence or absence of IL-1 $\beta$ . RNase-7 mRNA levels were measured by qPCR. **e** IL-1 $\beta$  induced

RNase-7 protein levels are not altered by NF- $\kappa$ B pathway inhibitors. IF staining of RNase-7 (middle panel) in inhibitor-pretreated hCECs compared to those treated with IL-1 $\beta$  alone. Scale bar: 100  $\mu$ M. **f, g** Knockdown of NF- $\kappa$ B1/p105 does not alter IL-1 $\beta$  induced RNase-7 levels. **f** NF- $\kappa$ B1/p105 siRNA does not affect RNase-7 mRNA levels. Cells transfected without or with indicated siRNA prior to incubation in the presence or absence of IL-1 $\beta$  were then analysed by qPCR for RNase-7 mRNA levels. The *p* value corresponds to the significance relative to the negative control. **g** Unchanged RNase-7 protein levels in NF- $\kappa$ B1/p105 siRNA transfected hCECs. Cells transfected without or with indicated siRNA prior to incubation with IL-1 $\beta$  were stained for RNase-7 (middle panel) and DAPI (lower panel). Scale bar 100  $\mu$ M. All data represent means  $\pm$  SEM of three samples repeated three times. *p* < 0.05

I $\kappa$ B- $\alpha$  or NF- $\kappa$ B1/p105. In response to a variety of stimuli, these molecules are phosphorylated and degraded, and subsequently lead to release and nuclear translocation of NF- $\kappa$ B dimers [16]. To examine the role of p50 in IL-1 $\beta$ -mediated expression of RNase-7, we silenced its precursor molecule, NF- $\kappa$ B1/p105 (see ESM, Online Resource 2B, 1 nM) in hCECs prior to treatment with IL-1 $\beta$  (10 ng/ml) for 3 h to study mRNA and for 24 h to study protein expression of RNase-7. The treatment with NF- $\kappa$ B1/p105 siRNA reduced the nuclear translocation and phosphorylation of NF- $\kappa$ B (data not shown) in response to IL-1 $\beta$ ; however, as shown in Fig. 3f and g, IL-1 $\beta$  induced RNase-7 mRNA and protein levels, respectively, remained unchanged. These findings indicate that the NF- $\kappa$ B pathway is not involved in IL-1 $\beta$ -mediated RNase-7 induction in hCECs.

MAPKs are required for RNase-7 regulation

Several stimuli, including IL-1 $\beta$ , induce the activation of MAPKs in various cell types [13]. To evaluate the effect of IL-1 $\beta$  on p38, JNK and ERK pathways, hCECs were stimulated for different durations (5, 15, 30, 60 and 120 min) with IL-1 $\beta$  (10 ng/ml). Western blotting analysis with monoclonal Abs against each MAPKs showed rapid phosphorylation at 5 min with maximal activation at 15 min (Fig. 4a). Notably, the phosphorylation of all three kinases was abrogated after the 60 min. Pre-incubation of hCECs with SB203580, SP600125 and PD98059 (selective inhibitors of p38, JNK and ERK respectively) (25 and 50  $\mu$ M each; 30 min) prior to IL-1 $\beta$  (10 ng/ml; 30 min) exposure resulted in reduced phosphorylation of p38, JNK

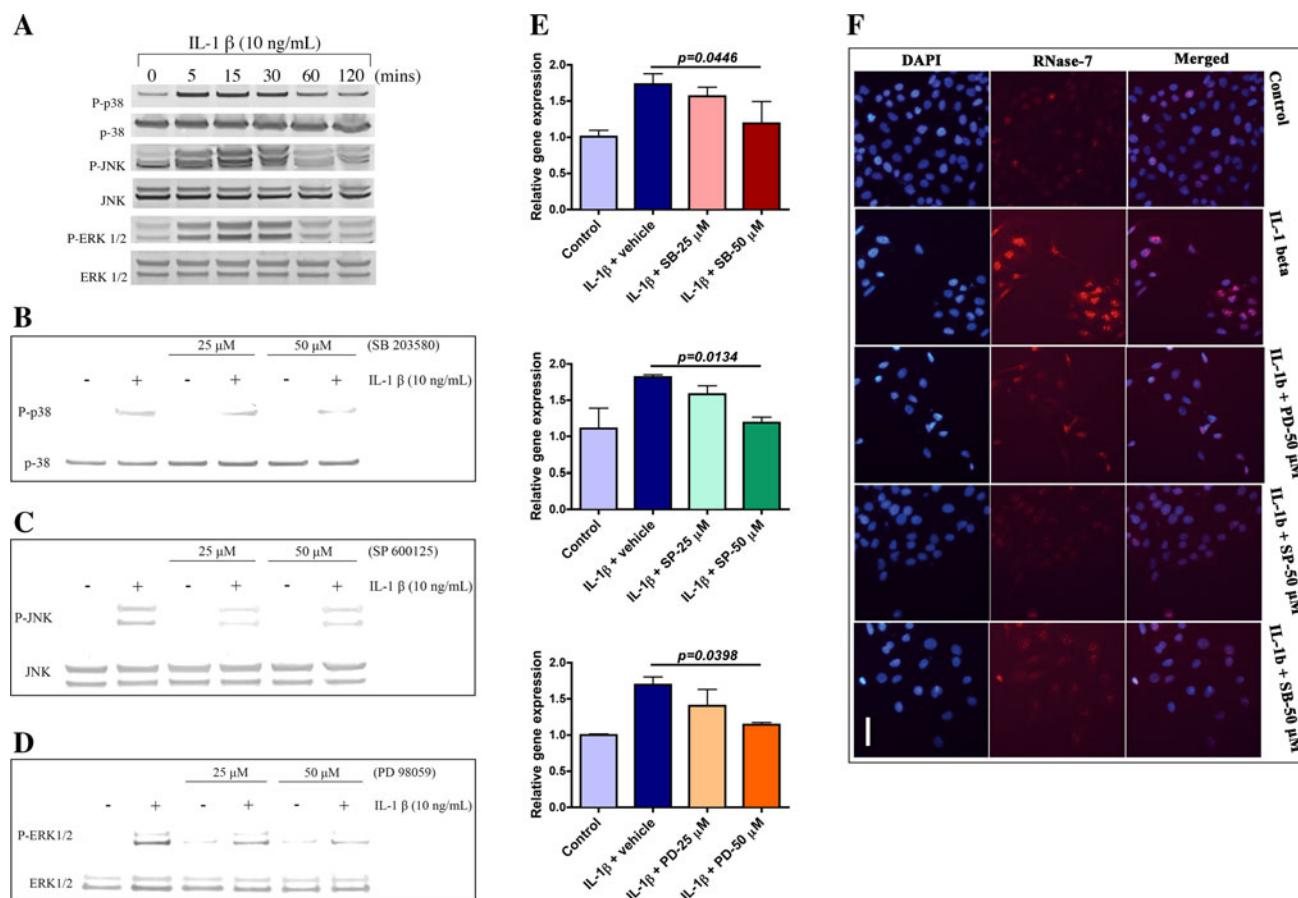


**Fig. 4** Mitogen-activated protein kinases are involved in RNase-7 mRNA expression. **a** Activation of MAPKs. Whole cell extract was prepared and then analysed using WB. **b–d** Effect of inhibitors on IL-1 $\beta$ -induced activation of p38, JNK and ERK. Whole cell extract was prepared post-treatment without or with indicated concentrations of SB203580. **b** SP600125. **c** PD98059 and **d** each prior to IL-1 $\beta$  exposure. Western blotting analysis was performed using indicated Abs. **e, f** Role of MAPKs in IL-1 $\beta$ -induced RNase-7 expression. **e** Blocking MAPKs reduces IL-1 $\beta$  induced RNase-7 mRNA levels. Cells are pretreated with inhibitors of p38 (top), JNK (middle) and

ERK (bottom) at indicated concentrations and then were incubated in absence or presence of IL-1 $\beta$ . RNase-7 mRNA levels were measured by qPCR. Data are presented as mean  $\pm$  SEM from three independent experiments with triplicate samples.  $p < 0.05$ . **f** Inhibitors of MAPKs reduce IL-1 $\beta$ -induced RNase-7 protein levels. Immunofluorescence staining was performed post-treatment without or with specified inhibitors at indicated concentration and then were incubated in absence or presence of IL-1 $\beta$  for 3 h. Scale bar 100  $\mu$ M. All data are representative of three independent experiments

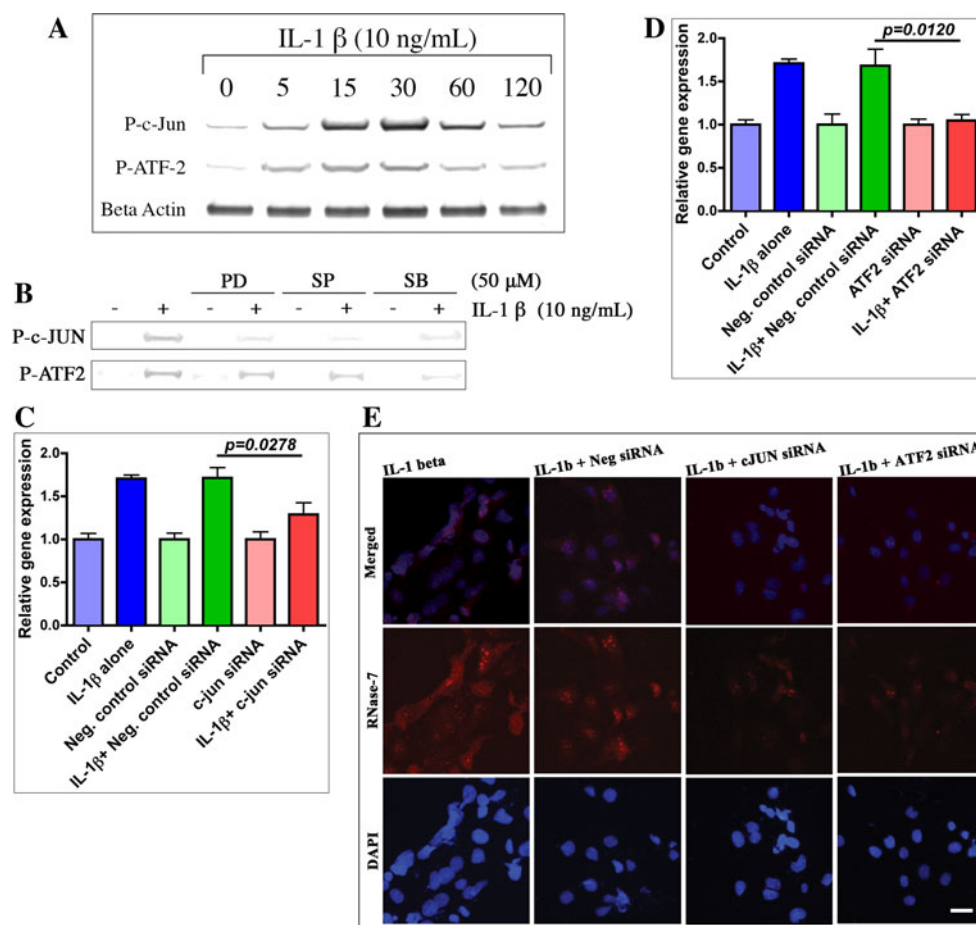


**Fig. 5** Essential role of c-Jun and ATF2 in RNase-7 expression. **a** IL-1 $\beta$  activates both c-Jun and ATF2. Cell lysate was prepared as described in SI and analysed using WB. **b** IL-1 $\beta$ /MAPKs mediate activation of c-Jun and ATF2. Whole cell extract prepared following treatment without or with indicated inhibitors each prior to IL-1 $\beta$  exposure was analysed using WB. **c–e** Role of c-Jun/ATF2 in RNase-7 expression. **c, d** Silencing c-Jun and ATF-2 reduces IL-1 $\beta$  induced RNase-7 mRNA expression. Following transfection without or with negative control or c-Jun **c** or ATF2 siRNAs **d** hCECs were incubated

in the presence or absence of IL-1 $\beta$  for 3 h. RNase-7 mRNA levels were analysed by qPCR and presented as mean value  $\pm$  SEM;  $n = 3$ . The  $p$  value was calculated relative to the negative control. **e** Reduction in IL-1 $\beta$  induced RNase-7 protein levels after silencing c-Jun and ATF2. Cells transfected without or with indicated siRNAs prior to incubation with IL-1 $\beta$  were stained for RNase-7 (Red middle panel) and DAPI (Blue lower panel). Scale bar 100  $\mu$ m. All the data are representative of three independent experiments

and ERK (Figs. 4b–d). This suggests that IL-1 $\beta$  plays a role in activation of MAPKs.

We next investigated whether MAPKs have any role in IL-1 $\beta$ -mediated RNase-7 mRNA regulation. Cells were treated with various doses of SB203580, SP600125 and PD98059 (25 and 50  $\mu$ M each), respectively, for 30 min before stimulation with IL-1 $\beta$  (10 ng/ml; 3 h). The level of IL-1 $\beta$ -induced RNase-7 mRNA was inhibited by the MAPK inhibitors in a dose-dependent fashion with 50  $\mu$ M final concentration showing the most significant effect (Fig. 4e). We also examined the involvement of MAPKs in RNase-7 protein expression mediated by IL-1 $\beta$ . Pretreatment of hCECs with the above-mentioned MAPK inhibitors (50  $\mu$ M each) for 30 min prior to IL-1 $\beta$  (10 ng/ml; 24 h) challenge resulted in equivalent reduction of

RNase-7 protein levels after blocking all three MAPKs (Figs. 4f). These results indicate that p38, JNK and ERK are required for RNase-7 expression in response to IL-1 $\beta$ .

#### Essential role of both c-Jun and ATF2 in RNase-7 expression

To elucidate the direct effect of IL-1 $\beta$  on these transcription factors (TF), we studied the phosphorylation activation of c-Jun and ATF2 using WB. Treatment of hCECs with IL-1 $\beta$  (10 ng/mL) for various durations (5, 15, 30, 60 and 120 min) has demonstrated rapid phosphorylation of both c-Jun and ATF2 at 5 min with maximal activation observed at 30 min, respectively. Interestingly, time-dependent reduction in c-Jun phosphorylation was noted



after a surge, whereas ATF2 showed sustained reduction in phosphorylation after 30 min, suggesting the differential roles of these two in IL-1 $\beta$ -mediated MAPKs-induced response.

To investigate the role of MAPKs in IL-1 $\beta$ -mediated c-Jun and ATF2 activation, we examined the effect of blocking ERK, JNK and p38 pathways on c-Jun and ATF2. As shown in Fig. 5b, IL-1 $\beta$ -induced c-JUN phosphorylation was significantly reduced in hCECs pretreated with JNK inhibitor and modestly reduced in those treated with ERK and p38 inhibitors, respectively, suggesting an essential role of JNK and minimal involvement of both ERK and p38 in c-Jun-mediated responses, whereas IL-1 $\beta$ -induced ATF2 activation was rapidly reduced after blocking p38 and partially reduced following ERK and JNK inhibitor pretreatment, respectively. This suggests that p38 plays a key role in IL-1 $\beta$ -ATF2-dependent innate responses; on the other hand, both ERK and JNK might play a secondary role.

To examine whether these TF's have any involvement in IL-1 $\beta$ -induced RNase-7 expression, we silenced both c-Jun and ATF2 individually using specific siRNAs at optimised concentration (see ESM; Online Resource 2C and 2D). RNAi knockdown of both c-Jun and ATF2 (1 nM; 24 h each) preceding IL-1 $\beta$  treatment (10 ng/ml; 3 h each) resulted in significant reduction of RNase-7 mRNA levels compared to negative control (10 nM; 24 h) treated hCECs (Fig. 5c and d). In addition, IL-1 $\beta$ -induced RNase-7 protein levels were also reduced in c-Jun and ATF2 siRNA pretreated hCECs compared to those treated with negative control. These results indicate the important role of both c-Jun and ATF2 in induction of RNase-7 expression by IL-1 $\beta$  in hCECs.

## Discussion

We report the constitutive presence of RNase-7, both protein and mRNA, in human OS cells and have localised its expression in the superficial cornea, conjunctiva and limbus. We also report several novel aspects of its expression, such as its rapid response and its signalling pathways (Fig. 6). This complements our previous studies [1, 2, 17, 18] and those of others [19, 20] in relation to defensin and cathelicidin families at the OS.

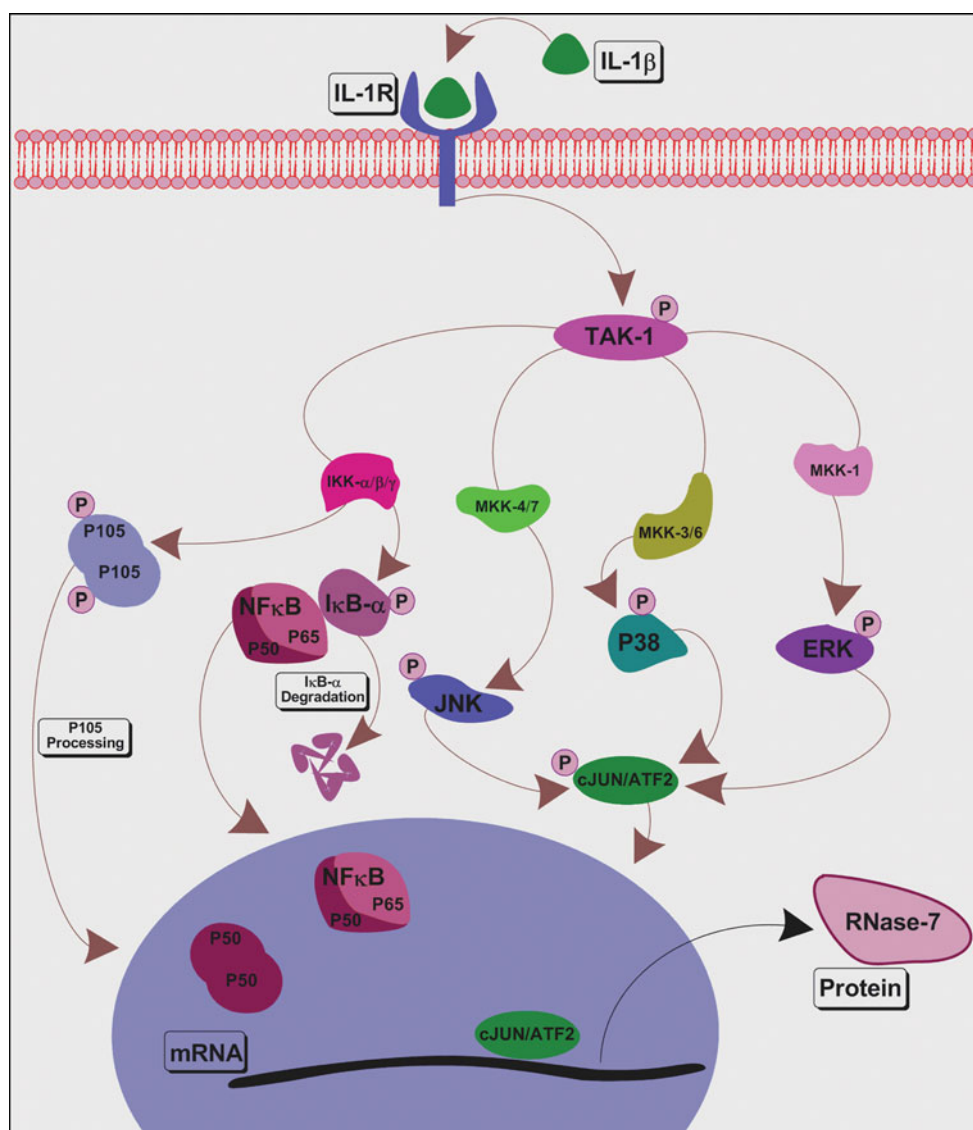
Human ocular epithelial cells respond to insult by producing cytokines such as IL-1 $\beta$ , which regulates the secretion of host defence peptides, growth factors and matrix metalloproteinases (MMPs) [15, 21, 22]. We have noted that IL-1 $\beta$  has a rapid but transient effect in RNase-7 induction in hCECs, suggesting a role in the immediate response of the ocular epithelium to inflammatory stimuli following infection or injury. Unlike other surfaces, AMP

participates in ocular host defence in cohort with a multitude of host defence molecules including lactoferrin, lysozyme and complement system. In addition, several studies have demonstrated the debilitating effect of upregulated host molecules on the corneal transparency and consequent sight-threatening problems such as glaucoma and cataract [23]. Therefore, it is expected that upregulation of RNase-7 at the OS, like other molecules, would be limited but sufficient to achieve the desired effect. This may be the reason why we were able to see only a 1.5-fold increase in mRNA following stimulation with IL-1 $\beta$ . Binding of IL-1 $\beta$  to its receptor IL-1R initiates a cascade of events including activation of both NF- $\kappa$ B and MAPK pathways [24, 25]. Further downstream, activation of these pathways induces the expression of cytokines or HBD-2 in various epithelia including OS [20]. As NF- $\kappa$ B and MAPK pathways are involved in expression of numerous genes of the innate immune system, we studied their role in IL-1 $\beta$ -induced RNase-7 expression.

Transforming growth factor  $\beta$  activated kinase-1 is activated by a variety of stimuli via the innate immune signalling pathways. However, its role at the OS has not been studied. Our results demonstrated that IL-1 $\beta$  induces activation of TAK-1 rapidly, but its effect fades away 60 min post-stimulation, suggesting a major role of TAK-1 at the OS. Knockdown of TAK-1 negatively affected the IL-1 $\beta$ -induced activation of I $\kappa$ B- $\alpha$ , JNK, ERK and p38. Yu et al. [26] have demonstrated similar effects of TAK-1-deficient murine fibroblasts on IL-1 $\beta$ -mediated NF- $\kappa$ B and MAPKs activation as well as IL-6 gene expression. Interestingly, there are no reports available that demonstrate the role of TAK-1 in IL-1 $\beta$ -induced AMP gene expression at any bodily surface. However, the only study that demonstrates the role of TAK-1 in HBD2 expression was in response to IL17A in human airway epithelial cells [27]. In this study, we demonstrated that RNAi silencing of TAK-1 resulted in significant reduction of the IL-1 $\beta$ -induced RNase-7 transcript and protein. Therefore, we propose that TAK-1 could play a central role in RNase-7 expression during inflammation.

Several reports have demonstrated the efficacy of SC-514 [28] and NAI [29] in deactivation of NF- $\kappa$ B-dependent gene expression. NAI has been shown to potently inhibit NF- $\kappa$ B activation and TNF- $\alpha$  production in vitro as well as in vivo [29]. Similarly, SC-514 was reported to strongly inhibit IL-1 $\beta$ -mediated IL-8 and p53 mRNA expression in the HepG2 cell line [28]. In this study, we have demonstrated that these two inhibitors were able to block the NF- $\kappa$ B pathway as well as effectively inhibit the mRNA expression of I $\kappa$ B- $\alpha$  and TNF- $\alpha$ . However, blocking the NF- $\kappa$ B pathway individually or in combination failed to inhibit IL-1 $\beta$ -induced RNase-7 mRNA and protein expression. Our work was robustly

**Fig. 6** Schematic diagram representing the signalling mechanism required for induction of RNase-7 by IL-1 $\beta$  in hCECs. Binding of IL-1 $\beta$  to membrane receptor IL-1R activates a cascade of signalling events including activation of TAK-1, NF- $\kappa$ B, p38, JNK and ERK. Further downstream, activation and nuclear translocation of transcription factors takes place, eventually leading to transcription of RNase-7. The results obtained in this study using siRNA or pharmacological inhibitors indicate that IL-1 $\beta$  induced RNase-7 expression is mediated via TAK-1-dependent MAPKs, but not NF- $\kappa$ B pathways



validated using blocking and siRNA experiments. Therefore, we can conclude that IL-1 $\beta$ -induced RNase-7 expression in hCECs is not dependent on NF- $\kappa$ B signaling. A similar dichotomy between the NF- $\kappa$ B and MAPK pathways to HBD-2 gene expression has been reported. In human gingival epithelial cells incubated with *F. nucleatum* [30], HBD2 expression is mediated via MAPKs, not NF- $\kappa$ B. Interestingly, *S. enteritidis* [31] or *H. pylori* [32] induced HBD2 expression is mediated via NF- $\kappa$ B, not AP-1. However, *C. albicans* [33] or *P. aeruginosa* [34] induces HBD-2 via both NF- $\kappa$ B and AP-1. Thus, it can be inferred that the transcriptional regulation of AMPs is dependent on the pathogen as well as the affected mucosal surface.

The unexpected redundancy of NF- $\kappa$ B prompted us to define the role of other IL-1 $\beta$ -mediated MAPK pathways in induction of RNase-7 at the OS. Kinetics of both MAPK activation and blocking studies demonstrated their role in IL-1 $\beta$  signalling. Interestingly, the effect of IL-1 $\beta$  on

RNase-7 mRNA and protein induction was significantly reduced after blocking p38, JNK and ERK in a dose-dependent manner. Based on the present evidence we suggest that IL-1 $\beta$  requires p38, JNK and ERK signalling to induce RNase-7 expression, unlike HBD2 [15].

Several reports have described the involvement of MAPK-AP1/cJun or/ATF2 axes in the induction of innate responses at mucosal surfaces. Steubesand et al. [33] demonstrated the role of c-Jun in *Candida albicans*-induced HBD-2 and -3 induction in human esophageal epithelium. Bauer et al. [35] demonstrated that both c-Jun and ATF-2 control the TNF- $\alpha$  regulation in human hepatoma cells by IL-1 $\beta$ . Our RNAi studies on the effect of c-Jun and ATF2 allow us to postulate that c-Jun and ATF2 are potential mediators of RNase-7 expression in hCECs.

The strength of this study is in the demonstration of the effects at both protein and mRNA levels and the high correlation of these with other target molecules in the

different experiments. We have also demonstrated in this study that blocking NF- $\kappa$ B, p38, JNK and ERK pathways with selective inhibitors resulted in reduced secretion of IL-6, IL-8 and TNF- $\alpha$  in response to IL-1 $\beta$ . In conclusion, the TAK-1-dependent MAPKs pathway could be exploited as a potential therapeutic modality for induction of RNase-7.

**Acknowledgments** We thank Mr. Naing Latt Tint and Mr. Manu Mathew for providing help in acquiring human tonsil and human ocular surface tissue, respectively, Dr. Hanif Suleman for immunofluorescent images processing, Dr. Sue Fox for helping us with BD-CBA assays, Dr. Felicity Rose for the gift of hCEC lines and Dr. Abdul Hameed for preparing the schematic diagram of RNase-7 signalling. This study was supported by grants from the British Eye Research Foundation (Fight for Sight) as PhD Studentship (to I.M.) and the Royal College of Surgeons of Edinburgh, UK.

## References

- Haynes RJ, Tighe PJ, Dua HS (1998) Innate defence of the eye by antimicrobial defensin peptides. *Lancet* 352(9126):451–452
- Haynes RJ, Tighe PJ, Dua HS (1999) Antimicrobial defensin peptides of the human ocular surface. *Br J Ophthalmol* 83(6):737–741
- Yount NY, Yeaman MR (2004) Multidimensional signatures in antimicrobial peptides. *Proc Natl Acad Sci USA* 101(19):7363–7368
- Verma C, Seebah S, Low SM, Zhou L, Liu SP, Li J, Beuerman RW (2007) Defensins: antimicrobial peptides for therapeutic development. *Biotechnol J* 2(11):1353–1359
- Rosenberg HF (2008) RNase A ribonucleases and host defense: an evolving story. *J Leukoc Biol*
- Harder J, Schroder JM (2002) RNase 7, a novel innate immune defense antimicrobial protein of healthy human skin. *J Biol Chem* 277(48):46779–46784
- Zhang J, Dyer KD, Rosenberg HF (2003) Human RNase 7: a new cationic ribonuclease of the RNase A superfamily. *Nucleic Acids Res* 31(2):602–607
- Torrent M, Badia M, Moussaoui M, Sanchez D, Nogues MV, Boix E (2010) Comparison of human RNase 3 and RNase 7 bactericidal action at the gram-negative and gram-positive bacterial cell wall. *FEBS J* 277(7):1713–1725
- Glaser R, Navid F, Schuller W, Jantschitsch C, Harder J, Schroder JM, Schwarz A, Schwarz T (2009) UV-B radiation induces the expression of antimicrobial peptides in human keratinocytes in vitro and in vivo. *J Allergy Clin Immunol* 123(5):1117–1123
- Gambichler T, Skrygan M, Tomi NS, Othlinghaus N, Brockmeyer NH, Altmeyer P, Kreuter A (2008) Differential mRNA expression of antimicrobial peptides and proteins in atopic dermatitis as compared to psoriasis vulgaris and healthy skin. *Int Arch Allergy Immunol* 147(1):17–24
- Reithmayer K, Meyer KC, Kleditzsch P, Tiede S, Uppalapati SK, Glaser R, Harder J, Schroder JM, Paus R (2009) Human hair follicle epithelium has an antimicrobial defence system that includes the inducible antimicrobial peptide psoriasin (S100A7) and RNase 7. *Br J Dermatol* 161(1):78–89
- Kida Y, Kobayashi M, Suzuki T, Takeshita A, Okamatsu Y, Hanazawa S, Yasui T, Hasegawa K (2005) Interleukin-1 stimulates cytokines, prostaglandin E2 and matrix metalloproteinase-1 production via activation of MAPK/AP-1 and NF-kappaB in human gingival fibroblasts. *Cytokine* 29(4):159–168
- Sato S, Sanjo H, Takeda K, Ninomiya-Tsuji J, Yamamoto M, Kawai T, Matsumoto K, Takeuchi O, Akira S (2005) Essential function for the kinase TAK1 in innate and adaptive immune responses. *Nat Immunol* 6(11):1087–1095
- Jang BC, Lim KJ, Paik JH, Kwon YK, Shin SW, Kim SC, Jung TY, Kwon TK, Cho JW, Baek WK, Kim SP, Suh MH, Suh SI (2004) Up-regulation of human beta-defensin 2 by interleukin-1beta in A549 cells: involvement of PI3K, PKC, p38 MAPK, JNK, and NF-kappaB. *Biochem Biophys Res Commun* 320(3):1026–1033
- McDermott AM, Redfern RL, Zhang B, Pei Y, Huang L, Proske RJ (2003) Defensin expression by the cornea: multiple signalling pathways mediate IL-1beta stimulation of hBD-2 expression by human corneal epithelial cells. *Invest Ophthalmol Vis Sci* 44(5):1859–1865
- Sun SC, Ley SC (2008) New insights into NF-kappaB regulation and function. *Trends Immunol* 29(10):469–478
- Abedin A, Mohammed I, Hopkinson A, Dua HS (2008) A novel antimicrobial peptide on the ocular surface shows decreased expression in inflammation and infection. *Invest Ophthalmol Vis Sci* 49(1):28–33
- McIntosh RS, Cade JE, Al-Abed M, Shanmuganathan V, Gupta R, Bhan A, Tighe PJ, Dua HS (2005) The spectrum of antimicrobial peptide expression at the ocular surface. *Invest Ophthalmol Vis Sci* 46(4):1379–1385
- McDermott AM (2004) Defensins and other antimicrobial peptides at the ocular surface. *Ocul Surf* 2(4):229–247
- Shin JS, Kim CW, Kwon YS, Kim JC (2004) Human beta-defensin 2 is induced by interleukin-1beta in the corneal epithelial cells. *Exp Mol Med* 36(3):204–210
- Cai S, Brandt CR (2008) Induction of interleukin-6 in human retinal epithelial cells by an attenuated Herpes simplex virus vector requires viral replication and NFkappaB activation. *Exp Eye Res* 86(2):178–188
- Fini ME, Stramer BM (2005) How the cornea heals: cornea-specific repair mechanisms affecting surgical outcomes. *Cornea* 24(8 Suppl):S2–S11
- Hazlett LD (2004) Corneal response to *Pseudomonas aeruginosa* infection. *Prog Retin Eye Res* 23(1):1–30
- Chowdhury TT, Salter DM, Bader DL, Lee DA (2008) Signal transduction pathways involving p38 MAPK, JNK, NFkappaB and AP-1 influences the response of chondrocytes cultured in agarose constructs to IL-1beta and dynamic compression. *Inflamm Res* 57(7):306–313
- Hanada T, Yoshimura A (2002) Regulation of cytokine signalling and inflammation. *Cytokine Growth Factor Rev* 13(4–5):413–421
- Yu Y, Ge N, Xie M, Sun W, Burlingame S, Pass AK, Nuchtern JG, Zhang D, Fu S, Schneider MD, Fan J, Yang J (2008) Phosphorylation of Thr-178 and Thr-184 in the TAK1 T-loop is required for interleukin (IL)-1-mediated optimal NF-kappaB and AP-1 activation as well as IL-6 gene expression. *J Biol Chem* 283(36):24497–24505
- Huang F, Kao CY, Wachi S, Thai P, Ryu J, Wu R (2007) Requirement for both JAK-mediated PI3K signalling and ACT1/TRAF6/TAK1-dependent NF-kappaB activation by IL-17A in enhancing cytokine expression in human airway epithelial cells. *J Immunol* 179(10):6504–6513
- Kishore N, Sommers C, Mathialagan S, Guzova J, Yao M, Hauser S, Huynh K, Bonar S, Mielke C, Albee L, Weier R, Graneto M, Hanau C, Perry T, Tripp CS (2003) A selective IKK-2 inhibitor blocks NF-kappa B-dependent gene expression in interleukin-1 beta-stimulated synovial fibroblasts. *J Biol Chem* 278(35):32861–32871

29. Tobe M, Isobe Y, Tomizawa H, Nagasaki T, Takahashi H, Hayashi H (2003) A novel structural class of potent inhibitors of NF-kappa B activation: structure-activity relationships and biological effects of 6-aminoquinazoline derivatives. *Bioorg Med Chem* 11(18):3869–3878
30. Krisanaprakornkit S, Kimball JR, Dale BA (2002) Regulation of human beta-defensin-2 in gingival epithelial cells: the involvement of mitogen-activated protein kinase pathways, but not the NF-kappaB transcription factor family. *J Immunol* 168(1):316–324
31. Ogushi K, Wada A, Niidome T, Mori N, Oishi K, Nagatake T, Takahashi A, Asakura H, Makino S, Hojo H, Nakahara Y, Ohsaki M, Hatakeyama T, Aoyagi H, Kurazono H, Moss J, Hirayama T (2001) *Salmonella enteritidis* FliC (flagella filament protein) induces human beta-defensin-2 mRNA production by Caco-2 cells. *J Biol Chem* 276(32):30521–30526
32. Boughan PK, Argent RH, Body-Malapel M, Park JH, Ewings KE, Bowie AG, Ong SJ, Cook SJ, Sorensen OE, Manzo BA, Inohara N, Klein NJ, Nunez G, Atherton JC, Bajaj-Elliott M (2006) Nucleotide-binding oligomerization domain-1 and epidermal growth factor receptor: critical regulators of beta-defensins during *Helicobacter pylori* infection. *J Biol Chem* 281(17):11637–11648
33. Steubesand N, Kiehne K, Brunke G, Pahl R, Reiss K, Herzig KH, Schubert S, Schreiber S, Folsch UR, Rosenstiel P, Arlt A (2009) The expression of the beta-defensins hBD-2 and hBD-3 is differentially regulated by NF-kappaB and MAPK/AP-1 pathways in an in vitro model of *Candida esophagitis*. *BMC Immunol* 10:36
34. Wehkamp K, Schwichtenberg L, Schroder JM, Harder J (2006) *Pseudomonas aeruginosa*- and IL-1beta-mediated induction of human beta-defensin-2 in keratinocytes is controlled by NF-kappaB and AP-1. *J Invest Dermatol* 126(1):121–127
35. Bauer I, Al Sarraj J, Vinson C, Larsen R, Thiel G (2007) Interleukin-1beta and tetradecanoylphorbol acetate-induced biosynthesis of tumor necrosis factor alpha in human hepatoma cells involves the transcription factors ATF2 and c-Jun and stress-activated protein kinases. *J Cell Biochem* 100(1):242–255